SEISMIC SIMULATIONS USING PARALLEL COMPUTING AND THREE-DIMENSIONAL EARTH MODELS TO IMPROVE NUCLEAR EXPLOSION PHENOMENOLOGY AND MONITORING

Arthur J. Rodgers, Eric Matzel, Michael E. Pasyanos, Anders Petersson, Bjorn A. Sjogreen, Caroline Bono, Oleg Vorobiev, Tarabay H. Antoun, Ilya N. Lomov, William R. Walter, and Stephen C. Myers

Lawrence Livermore National Laboratory

Sponsored by National Nuclear Security Administration

Contract No. DE-AC52-07NA27344

ABSTRACT

The development of accurate numerical methods to simulate wave propagation in three-dimensional (3D) earth models and advances in computational power offer exciting possibilities for modeling the motions excited by underground nuclear explosions. This presentation will describe recent work to use new numerical techniques and parallel computing to model earthquakes and underground explosions to improve understanding of the wave excitation at the source and path-propagation effects. Firstly, we are using the spectral element method (SEM, SPECFEM3D code of Komatitsch and Tromp, 2002) to model earthquakes and explosions at regional distances using available 3D models. SPECFEM3D simulates anelastic wave propagation in fully 3D earth models in spherical geometry with the ability to account for free surface topography, anisotropy, ellipticity, rotation and gravity. Results show in many cases that 3D models are able to reproduce features of the observed seismograms that arise from path-propagation effects (e.g., enhanced surface wave dispersion, refraction, amplitude variations from focusing and defocusing, tangential component energy from isotropic sources). We are currently investigating the ability of different 3D models to predict path-specific seismograms as a function of frequency. A number of models developed using a variety of methodologies are available for testing. These include the WENA/Unified model of Eurasia (e.g. Pasyanos et al 2004), the global CUB 2.0 model (Shapiro and Ritzwoller, 2002), the partitioned waveform model for the Mediterranean (van der Lee et al., 2007) and stochastic models of the Yellow Sea Korean Peninsula region (Pasyanos et al., 2006). Secondly, we are extending our Cartesian anelastic finite difference code (WPP of Nilsson et al., 2007) to model the effects of free-surface topography. WPP models anelastic wave propagation in fully 3D earth models using mesh refinement to increase computational speed and improve memory efficiency. Thirdly, we are modeling non-linear near-source shock wave propagation with GEODYN, an Eulerian Godunov finite-difference code (Antoun et al., 2001). This code accounts for shock wave propagation and a variety of effects, including cavity formation, rock fracture and plastic deformation. We are exploring the coupling of GEODYN to WPP to propagate motions from the near-source (non-linear) region to the (linear anelastic) region where seismic observations are made at local, regional and teleseismic distances. This effort has just begun and we show preliminary results in this paper. These simulation tools are supported by massively parallel computers operated by Livermore Computing.

Report Documentation Page

Form Approved
OMB No. 0704-0188

1. REPORT DATE	2. REPORT TYPE	3. DATES COVERED
SEP 2008		**00-00-2008 to 00-00-2008**

4. TITLE AND SUBTITLE	5a. CONTRACT NUMBER
Seismic Simulations Using Parallel Computing and Three-Dimensional Earth Models to Improve Nuclear Explosion Phenomenology and Monitoring	5b. GRANT NUMBER
	5c. PROGRAM ELEMENT NUMBER
6. AUTHOR(S)	5d. PROJECT NUMBER
	5e. TASK NUMBER
	5f. WORK UNIT NUMBER
7. PERFORMING ORGANIZATION NAME(S) AND ADDRESS(ES) **Lawrence Livermore National Laboratory,PO Box 808,Livermore,CA,94551-0808**	8. PERFORMING ORGANIZATION REPORT NUMBER
9. SPONSORING/MONITORING AGENCY NAME(S) AND ADDRESS(ES)	10. SPONSOR/MONITOR'S ACRONYM(S)
	11. SPONSOR/MONITOR'S REPORT NUMBER(S)

12. DISTRIBUTION/AVAILABILITY STATEMENT
Approved for public release; distribution unlimited

13. SUPPLEMENTARY NOTES
Proceedings of the 30th Monitoring Research Review: Ground-Based Nuclear Explosion? Monitoring?Technologies, 23-25 Sep 2008, Portsmouth, VA sponsored by the National Nuclear Security Administration (NNSA) and the Air Force Research Laboratory (AFRL)

14. ABSTRACT
see report

15. SUBJECT TERMS

16. SECURITY CLASSIFICATION OF:			17. LIMITATION OF ABSTRACT	18. NUMBER OF PAGES	19a. NAME OF RESPONSIBLE PERSON
a. REPORT **unclassified**	b. ABSTRACT **unclassified**	c. THIS PAGE **unclassified**	**Same as Report (SAR)**	**10**	

OBJECTIVES

Improvements in numerical methods to simulate wave phenomena in three-dimensional (3D) heterogeneous geologic materials, implementation of these algorithms on parallel computers and the inexorable increase of computational power offer exciting possibilities for the ability to simulate wave propagation for improving understanding of the nuclear explosion source and nuclear explosion monitoring. The objective of this study is to describe the development of new seismic wave modeling capabilities at Lawrence Livermore National Laboratory (LLNL) and articulate how these capabilities can improve understanding of observed seismic waves, particularly source excitation and propagation effects. Nuclear explosion monitoring based on seismic data ultimately relies on understanding the fundamentals of excitation of waves in the earth by the high-energy nuclear explosion source, shock-wave propagation in the near-source region and subsequent elastic wave propagation, including interaction with near-source geology and topography and path propagation. We are applying newly developed numerical methods and high performance computational resources to improve knowledge of observable effects on seismograms due to propagation in realistic 3D earth models and geologic materials.

RESEARCH ACCOMPLISHED

This effort covers three areas of research: 1) simulation of regional distance (< 1500 km) seismograms at intermediate periods (0.02-0.1 Hz) with the spectral element method (SEM); 2) simulation of realistic free-surface topography with our Cartesian anelastic finite difference code (WPP); and 3) the simulation of non-linear shock wave phenomena in realistic geologic materials (GEODYN) and the coupling of non-linear motions to our linear anelastic code (WPP). All these efforts rely on massively parallel computer systems at LLNL.

Simulations of Seismic Wave Propagation in 3D Models at Regional Distances and Intermediate Periods

Researchers in the academic and nuclear monitoring communities have vigorously developed 3D seismic velocity models based on various seismic tomographic methods. Computational methods for seismic wave propagation using parallel computers allow us to compute synthetic seismograms in 3D models for intermediate periods (≥ 10 seconds) at regional distances (< 1500 km). To do this, we are using the spectral element method (SEM) code SPECFEM3D (Komatitsch and Vilotte, 1998; Komatitsch and Tromp, 1999; Komatitsch et al., 2000). This code computes the response of the earth to arbitrary forcing in spherical geometry with fully 3D seismic velocity (including anisotropy) and density variations. The code also handles the effects of free-surface topography and bathymetry, ellipticity, rotation and self-gravitation. We have modified the code to handle a simple, but general 3D model format.

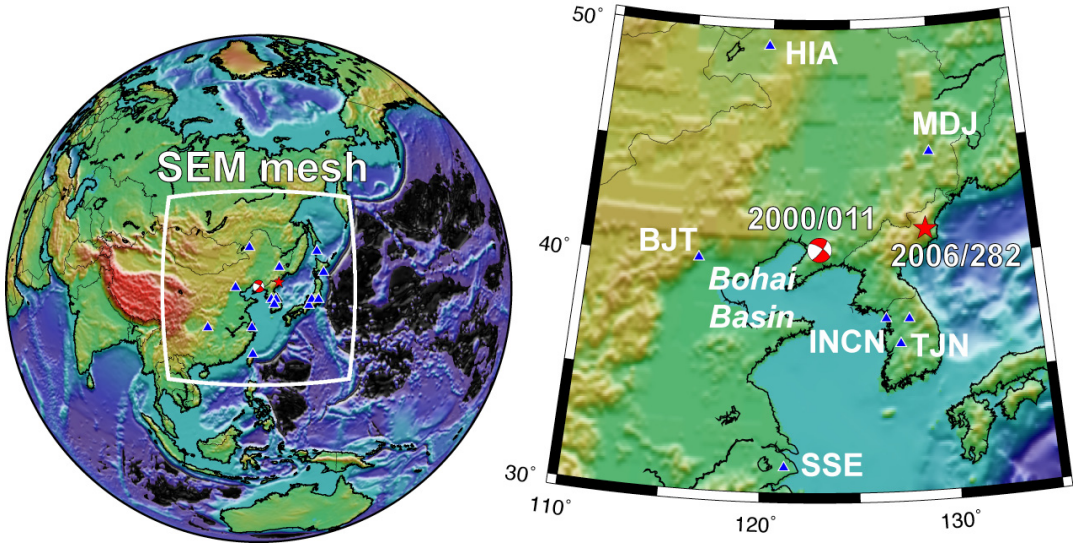

Figure 1. (left) SPECFEM3D computational domain for regional simulations of events in East Asia. (right) Map showing the locations of the January 11, 2000 (2000/011) earthquake and October 9, 2006, (2006/282) North Korean nuclear explosion along with regional broadband stations that recorded the events.

We have used this code to compute synthetics seismograms for the January 11, 2000, moderate (M_W ~ 5) earthquake in the Korean Peninsula and the (M_W ~ 4) October 9, 2006, North Korean nuclear explosion. Figure 1 (left) shows SPECFEM3D computational domain at the surface (white box) covering a 45° "chunk" (solid angle) of the earth. Figure 1 (right) shows a map of the events and recording stations for these two events. Focal parameters for the earthquake were obtained from waveform modeling using 1D methods.

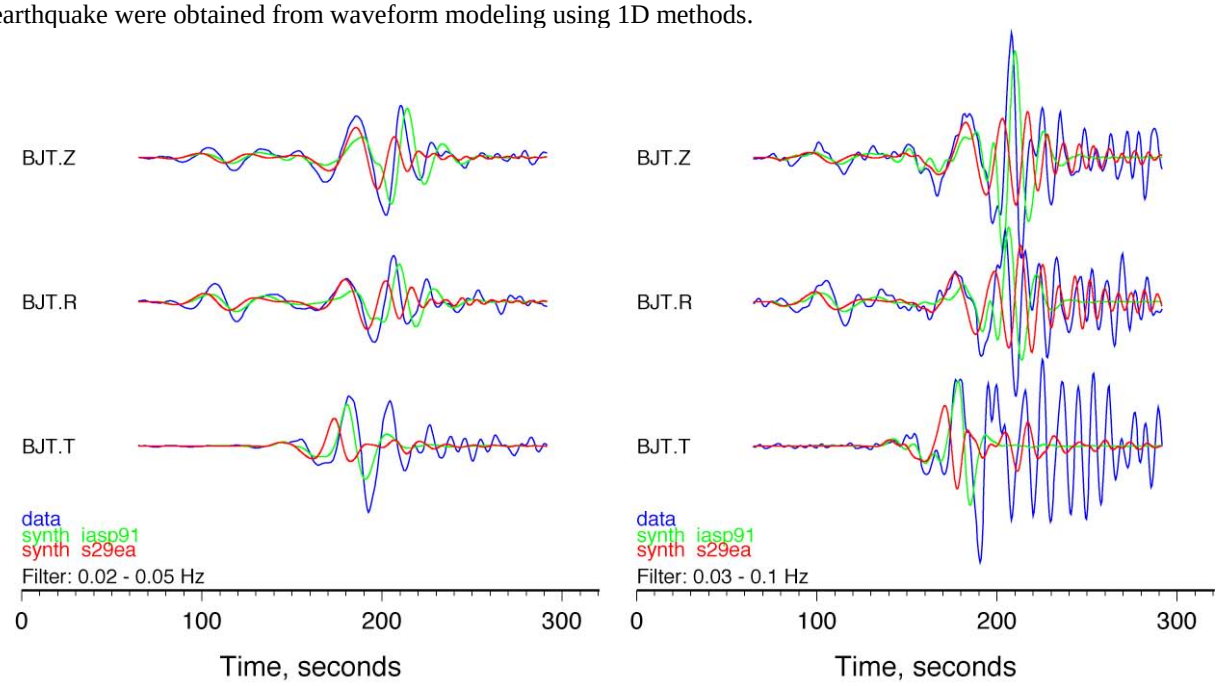

Figure 2. Observed (blue) and synthetic seismograms for the 2000/011 earthquake at station BJT for the iasp91 (green) and *s29ea+CRUST2.0* (red) models filtered 0.02-0.05 Hz (left) and 0.03-0.1 Hz (right).

Figure 2 shows the observed and synthetic waveforms for the 2000/011 earthquake at station BJT (Beijing, China) filtered in two different bands: 0.02–0.05 and 0.03–0.07 Hz (left and right, respectively). Synthetics were computed for two models: the iasp91 1D model (Kennett and Engdahl, 1991) shown as the green synthetics and the *s29ea+CRUST2.0* 3D model (Kustowski et al., 2008) shown as the red synthetics. Calculations resulted in seismograms that were resolved in the frequency band 0.0–0.12 Hz and took about 4 hours on 64 CPU's of a modest Linux cluster operated by the Ground-Based Nuclear Explosion Monitoring (GNEM) Program at LLNL. All calculations included the effects of surface topography, bathymetry and ellipticity. This event was moderately large (M_W ~ 5.0) and had good signal-noise across a broadband. Note that for 0.02–0.05 Hz (20–50 second periods) the observed and synthetic waveforms are very simple with clear Pnl, Rayleigh and Love waves. At these periods the synthetics match the observed waveforms with the iasp91 model showing a slightly better fit to the phase and amplitudes of the data. However, including slightly higher frequencies (0.1 Hz or 10 seconds periods) the observed waveforms show much greater complexity, especially the surface waves. This complexity is likely due to interaction with the Bohai Basin (Figure 1). Note that the Rayleigh wave is strongly dispersed and the later part of the Love wave shows a long duration with little dispersion. The *s29ea+CRUST2.0* 3D model captures some of the more complex surface waveform, mostly in the Rayleigh wave. As expected at intermediate frequencies (0.02–0.07 Hz or 14–20 second periods) the observed waveforms are less complex.

This example (Figure 2) demonstrates the challenge for waveform-based monitoring of small-to-moderate sized events (M_W 3.5–4.5). These events radiate very little long-period energy and are often observed where the surface waves only have signals above the noise for intermediate periods (e.g., 0.03–0.1 Hz or 10–33 seconds). For waveform analysis at intermediate periods seismologists require good constraints on the path-specific structure. We are performing calculations with a variety of available 3D models to determine the performance of models for predicting observed waveforms as a function of frequency content. It is important to quantify the performance of 3D

models so that they may be used as starting models for waveform-based tomography, such as adjoint methods (Tromp et al., 2005; Liu and Tromp, 2006).

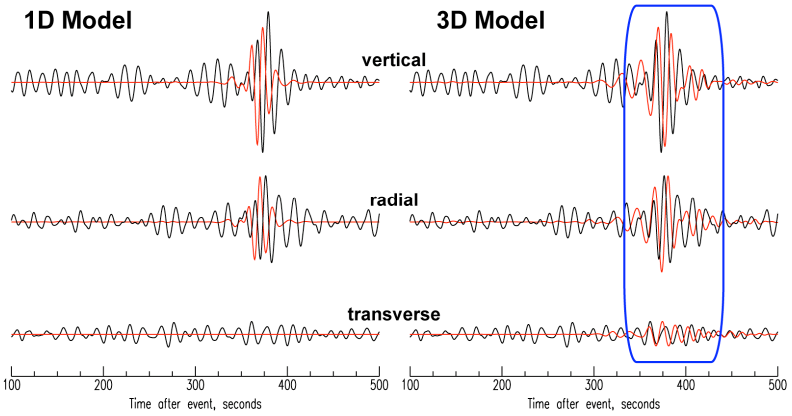

Figure 3. Observed (black) and synthetic (red) three-component seismograms for the 1D iasp91 (left) and 3D CUB2.0 (right) models. Both data and synthetics are filtered 0.05-0.1 Hz (10-20 second periods).

As another example of the effects of known 3D structure on intermediate period surface waves we show the observed and synthetic waveforms for the October 9, 2006, North Korean nuclear test at station BJT. The path to BJT passes through the northern edge of the Bohai Basin, similar to the path for the 2000/011 earthquake (Figure1). The synthetics for the 1D iasp91 and 3D *CUB2.0* model (Shapiro and Ritzwoller, 2002) are shown in Figure 3. While the signal-to-noise ratio of the transverse component at the expected time window of the surface wave is about 1:1 or slightly higher, the 3D synthetic predicts some energy that is not present in the synthetics for a 1D model. This illustrates how the refraction of surface waves by 3D structure, such as sedimentary basins, can cause rotation of energy from a purely isotropic source from the radial to the transverse component. Such wave propagation effects may bias estimates of source parameters for explosion sources such as seismic moment (and consequently explosive yield) and deviatoric moment tensor components.

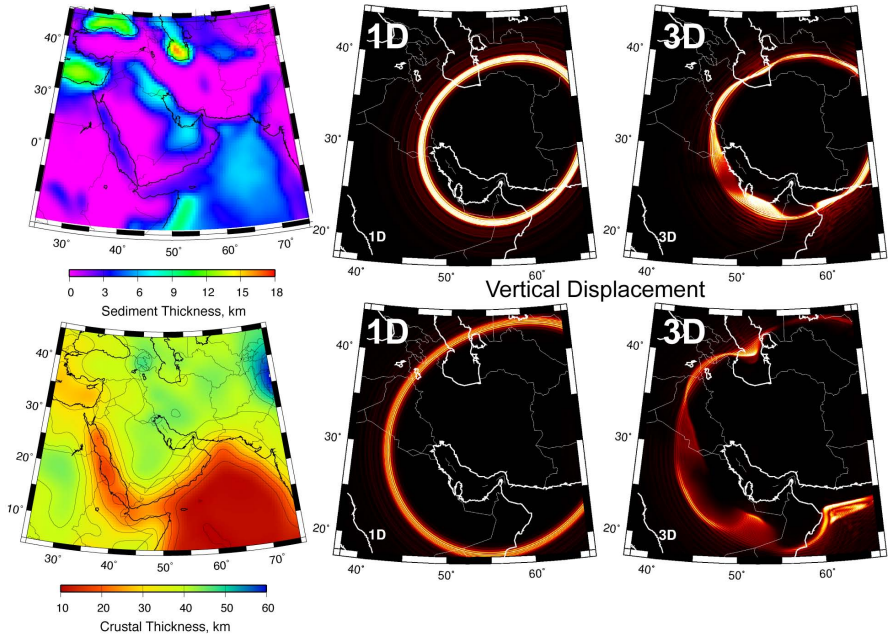

Figure 4. WENA 3D model properties across the Middle East: sediment thickness (top left) and crustal thickness (bottom left). Snapshots of vertical ground displacements showing Rayleigh wave propagation for an isotropic source using an average 1D model (center) and the WENA 3D model (right).

Finally, we performed large-scale simulations of regional seismic wave propagation in the Middle East using our anelastic finite difference code (WPP, described below). We modeled the M_W 6.25, February 22, 2005, Kerman earthquake using an average 1D model and the 3D WENA model of Pasyanos et al. (2004). The WENA model represents 3D crustal and upper mantle structure with 1° resolution and reveals the known sedimentary and crustal structure of the Middle East (Figure 4, left). For simplicity of illustration, we compare the wave propagation excited by an isotropic source using the 1D and WENA 3D models (Figure 4, center and right, respectively). The vertical displacement wavefields are shown at two different time steps in the calculations. Notice the dramatic timing, amplitude and dispersion asymmetries in the 3D model compared to the 1D model. These effects are confirmed by observations of long-duration intermediate period surface waveforms for events in the Zagros Mountains and Iranian Plateau recorded in the eastern Arabian Peninsula along the Persian/Arabian Gulf coast.

Note that the simulations shown in Figure 4 required nearly 4 billion grid points for density, seismic velocities and quality factors covering a volume 3,000 km by 3,000 km by 400 km (depth) at 1,000-m resolution. The calculations took nearly 50,000 CPU-hours, taking nearly two days on 1,024 CPU's of the Thunder Linux cluster at LLNL. The simulations resulted in seismograms valid to 0.1 Hz (10 second periods).

Simulation of Seismic Wave Propagation with Realistic Free Surface Topography

LLNL recently developed a new parallel finite difference code for simulating anelastic wave propagation. The algorithm uses a node-center second-order discretization, described by Nilsson et al. (2007). The code, called WPP, is open source and available at https://computation.llnl.gov/casc/serpentine/index.html. Currently, the code handles fully 3D variations in seismic wave speeds and density, both acoustic and elastic wave propagation and attenuation with quality factors for P- and S-waves. The code allows for mesh refinement for memory and computational efficiency. As the resolvable frequency of seismic events increases, the corresponding wavelength of the seismic wave motion decreases requiring finer discretization and more grid points (and memory). For frequencies above about 0.5 Hz, effects of non-planar topography become increasingly important (Figure 5). We are currently extending the WPP code to accurately satisfy the free surface boundary conditions on realistic non-planar topography. This will be accomplished by using an energy conserving, summation-by-parts, finite difference discretization of the elastic wave equation on a curvilinear grid (Appelo and Petersson, 2008).

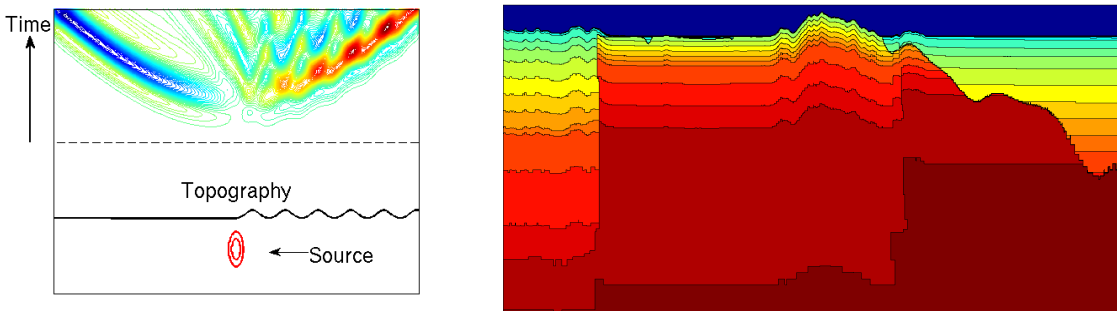

Figure 5. (left) Vertical displacement time history along the surface due to an isotropic point source below the surface. Note the effects of topography on the right side of the domain. (right) Compressional velocity (V_P) in an east-west cross-section of the San Francisco Bay area going through Mt. Tamalpais. The scale goes from 5,000 m/s (dark red) to 0 m/s (dark blue). The cross section extends to a depth of 10 km below sea level.

Since the curvilinear formulation involves about nine times more arithmetic operations per grid point than its Cartesian counterpart, the computational grid will be made Cartesian below some fixed elevation. As is visible in Figure 5 (right), the compressional wave speed (V_P) increases drastically with depth and is commonly about eight times larger below the Moho discontinuity (at about 30 km depth) than in sedimentary basins near the free surface. The propagation speed for shear waves has similar depth dependence, but the ratio between the two speeds depends on the material type (sediment, hard rock, etc.). Since the wavelength of elastic waves is proportional to the wave speed, structured mesh refinement (where the mesh gets coarser at depth) will be used to keep the grid size in approximate parity with the wavelength. Furthermore, since there is such a large change in wave speeds from the

surface to the bottom of the computational domain, mesh refinement will significantly reduce the total number of grid points and also allow the explicit time-stepping to use a much larger time step (improving computational efficiency). To guarantee stability of the time-stepping scheme in the presence of mesh refinement, we will use a newly developed energy conserving coupling of the solution across mesh refinement boundaries. For simplicity, only factor-of-two refinements are allowed and all mesh refinement boundaries must be horizontal. The latter restriction allows for a two-dimensional decomposition of the computational domain where each processor has a "pencil"-shaped domain from the topography at the top to the far-field boundary at the bottom. This layout allows for efficient load balancing on parallel machines and eliminates the need for expensive all-to-all communications.

The influence of topography is illustrated in Figure 6, where we show the response due to a vertically propagating shear wave impinging on a 3-D Gaussian hill. In this case, the material is homogeneous, a free surface boundary condition is imposed on the curved top surface, and periodic boundary conditions are used in the horizontal directions. The traces show displacement time histories at the surface along a densely sampled line passing through the center of the Gaussian hill. For a flat free surface, the horizontal component would only have one pulse corresponding to the arrival of the vertically propagation wave; the vertical component would be identically zero. In comparison, the curved topography induces reflected P- and S-waves, which also induce a vertical component to the motion.

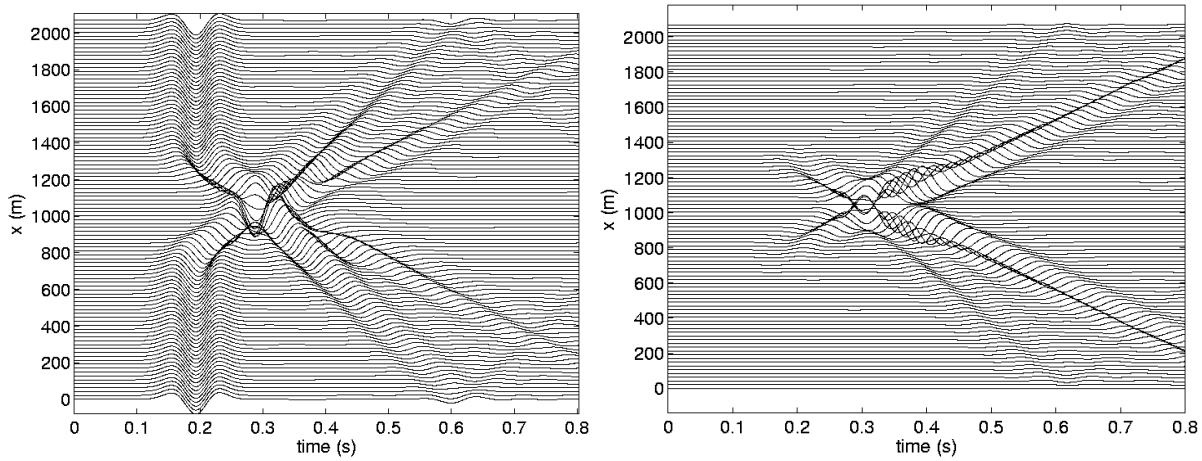

Figure 6. Horizontal (left) and vertical (right) displacement time histories along a line through the center of the Gaussian hill.

Simulation of Non-Linear Hydrodynamics with GEODYN and Coupling to WPP

The high energy density of chemical and nuclear explosions causes irreversible processes (e.g., vaporization, cavity creation and plastic deformation) in geologic materials near the source before stimulating seismic waves beyond the elastic radius. In order to simulate ground motions emerging from buried explosions, we must account for these processes including a complete thermodynmical treatment of the energy involved in these processes. Source emplacement conditions are known to have dramatic effects on the excitation of seismic waves that ultimately must be accounted for in yield estimates from seismic amplitudes and earthquake-explosion discriminants. The challenges of site-specific yield scaling relationships and the transportability of high-frequency regional discriminants can be traced to emplacement conditions and physical properties of geologic materials at the source.

The subject of this effort is to develop and illustrate a coupling approach between the non-linear GEODYN hydrodynamics code (Antoun et al., 2001) and the linear anelastic wave propagation code WPP, described above (Nilsson et al., 2007). GEODYN is a nonlinear Eulerian wave propagation code with adaptive mesh refinement (Antoun et al., 2001; Lomov and Rubin, 2003). The GEODYN code can handle large material deformations and phase transitions such as melting, vaporization, porous compaction and material damage. In the limit of low compressions and temperatures GEODYN can be applied to model linear waves in solid media, albeit at significant numerical cost over conventional anelastic finite difference methods. The code is not very efficient for handling linear waves since it carries around a lot of extra variables and performs calculations that are not needed for linear (elastic) wave propagation. WPP, on the other hand, cannot handle permanent deformations and uses a simple

scheme to model inelastic effects on the large scale (Liu and Archuleta, 2006). The purpose of this study (which has only just begun) is to couple the two codes to model the non-linear behavior of the near-source region with the full physics capabilities of GEODYN and pass these motions to WPP in an overlapping region in order to propagate the seismic waves to local, regional, and/or teleseismic distances. The basic idea of coupling is shown schematically in Figure 7.

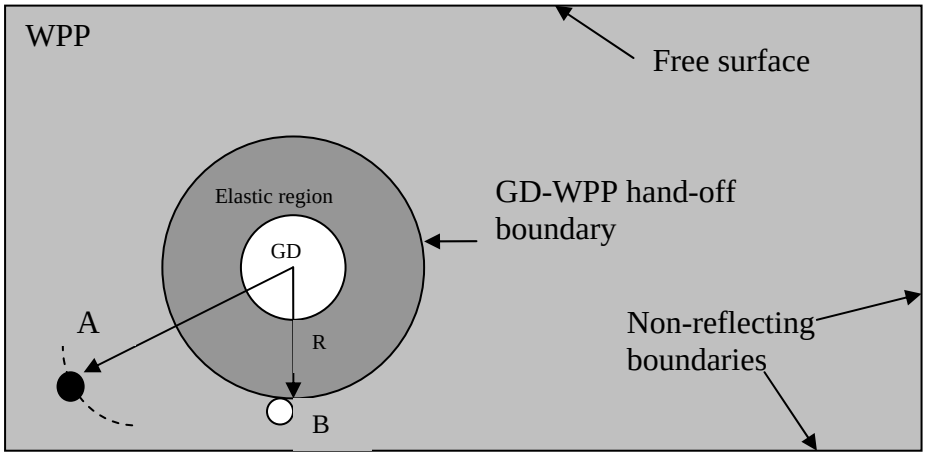

Figure 7. Conceptual illustration of the coupling between the nonlinear source region from GEODYN (GD) to WPP. The GEODYN domain extends to radius R (dark gray region), while the WPP domain covers a larger entire volume.

GEODYN can compute motions in 1D (spherically symmetric), 2D, 2.5D (2D axisymmetric) or fully 3D domains. Figure 7 describes a spherical source modeled in a 1D GEODYN calculation that was passed to a 3D WPP calculation. Material displacement inside the volume within the hand-off radius R was overwritten with pre-calculated 1D GEODYN data. One of the most important applications for GEODYN is the accurate simulation of ground motion due to underground explosions. Experimental data on spherical waves generated in situ by underground explosions published in open literature are scarce and are not always available with good geotechnical characterization of the emplacement rock. For this study, we chose to use data from a series of chemical high-explosive (HE) experiments in limestone performed in Kirghizia in 1960 (Murphy et al., 1997) to illustrate the code-coupling approach. The generic strength model described in Vorobiev (2008) was used in GEODYN to model 0.5% porous limestone. Experimental measurements of ground motion at different distances from the shot point were reported by Murphy et al. (1997). The explosions and motion recordings reported in this study were conducted in the subsurface in essentially rock whole-space conditions, making them ideal for our simulation experiments.

Figure 8 shows the vertical component displacement time histories calculated in 1D GEODYN (blue) and passed to WPP (red) at the boundary of the hand-off region (point B in Figure 7). The spatial resolution used in GEODYN was 6 cm and the space resolution used in 3D WPP was 1 m, allowing for resolution to about 100 Hz. Elastic constants used in WPP were chosen to match initial moduli for the generic limestone. Note that the amplitude and phase agree very well.

Figure 9 shows peak displacements as a function of range calculated by 1D GEODYN and 3D WPP codes. The 1D GEODYN calculations agree very well with experimentally measured values of peak velocity (crosses for point measurements taken from Figure 8 of Murphy et al., 1997). The peak displacements computed with WPP agree well with the GEODYN calculations when a fine grid spacing of 1 meter is used. However, the WPP peak displacements attenuate faster than 1/R when a grid spacing of 4 meters is used. This demonstrates that one must rigorously evaluate the numerical resolution of such calculations to be confident that numerical dispersion is minimized.

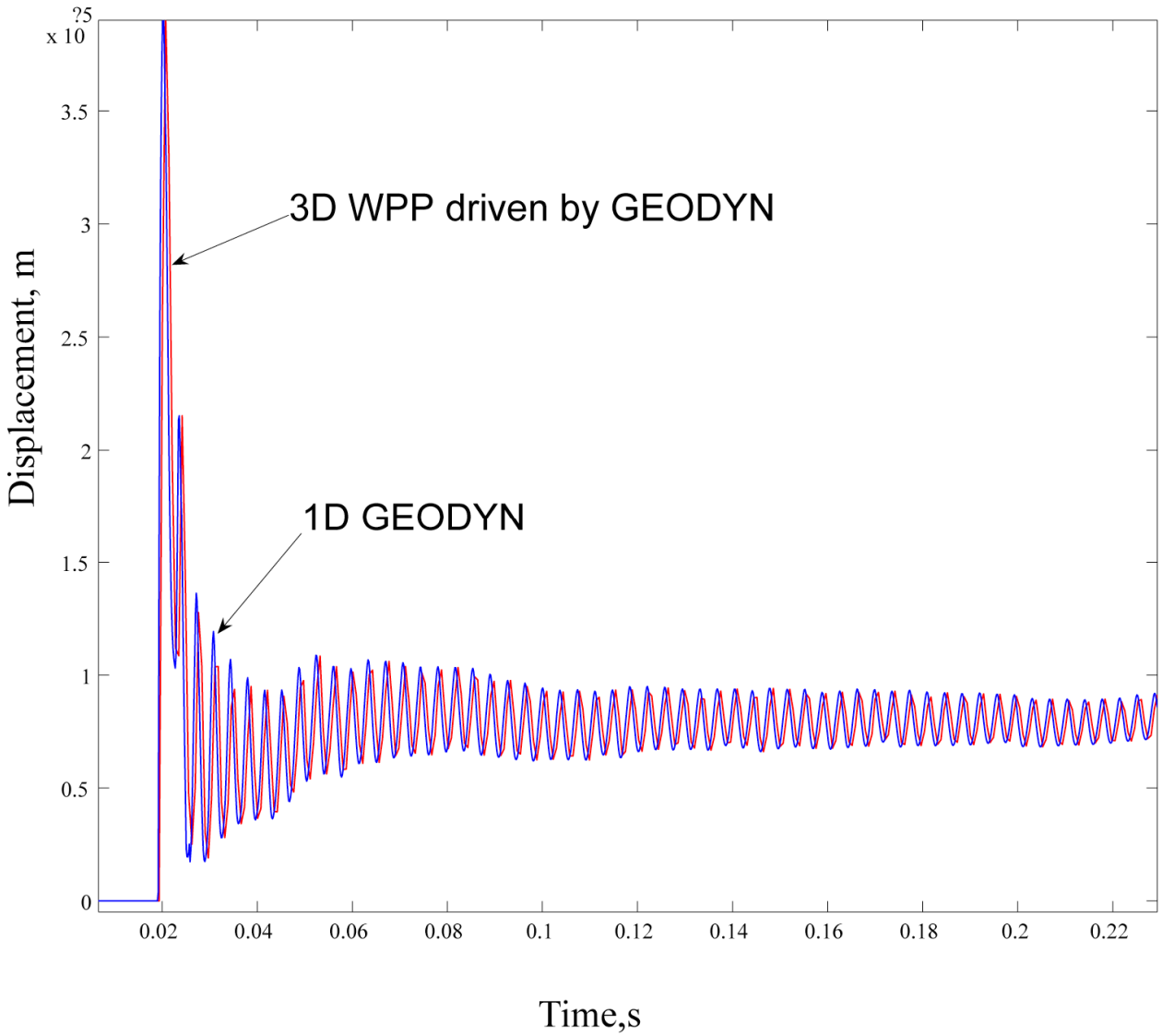

Figure 8. Vertical component displacement time history at the boundary of the hand-off region (point B in Figure 7) for the 3D WPP (red solid line) and 1D GEODYN (blue dotted line).

CONCLUSIONS AND RECOMMENDATIONS

Recent development of numerical methods for simulation of the 3D seismic wave excitation and propagation, coupled with ever-increasing computational power are offering exciting new capabilities for improving knowledge of seismic wave phenomenology for nuclear explosion monitoring. In this study, we demonstrated several efforts underway at LLNL that promise to advance capabilities for various aspects of seismic wave simulation.

The SEM code, SPECFEM3D, models seismic wave propagation in spherical geometry including important effects (e.g., 3D heterogeneity, anisotropy, free surface topography, ellipticity). This code allows us to compute intermediate period seismograms (periods greater than about 10 seconds) at regional distance (up to about 1500 km). We are using this code to test current available 3D seismic models. This code will be used in another study to exploit finite frequency sensitivity kernels for seismic waveform tomography based on adjoint methods (Savage et al., these Proceedings).

We are improving our Cartesian anelastic finite difference code (WPP) to add the effects of free-surface topography. The method will rely on a summation-by-parts principle and has been proven in research codes. The production

version of the WPP (version 2.0) will include the effects of free-surface topography and other improvements. Note that WPP is an open source code and can be downloaded from LLNL.

The coupling of our non-linear hydrodynamics code, GEODYN, with WPP will allow us to simulate ground motions from underground nuclear explosions including an accurate representation of the important near-source effects of cavity formation, melting, yielding, plastic deformation, porous compaction, and material damage all in a consistent thermodynamic framework. While many details remain to be sorted out, we have made good progress in the short time that we have been working on this effort.

These efforts involve complex numerical codes running on massively parallel computers. LLNL has significant experience in parallel code development as well as the computational resources to enable simulations of relevance to the nuclear explosion source phenomenology and monitoring investigations.

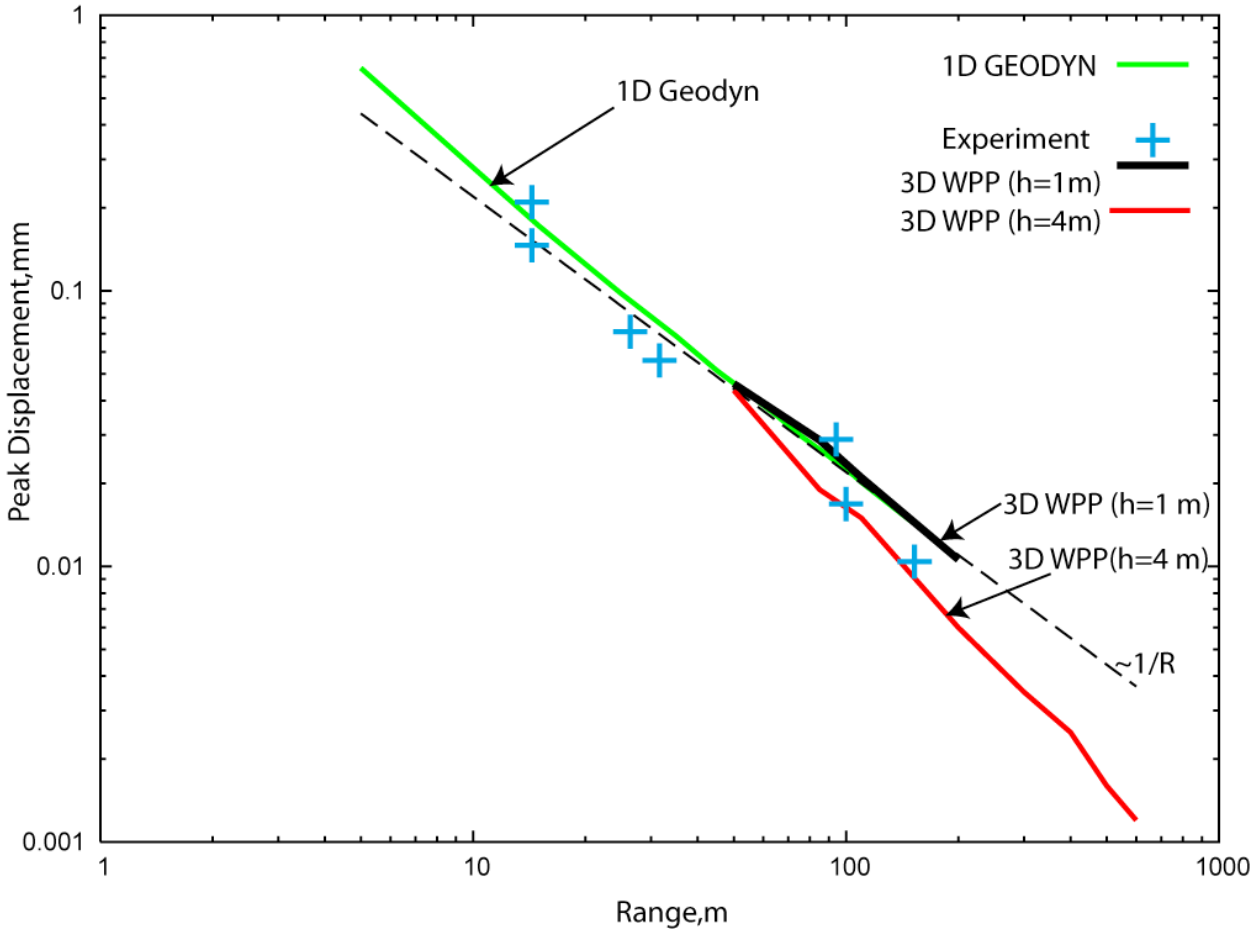

Figure 9. Peak displacement versus range for a chemical HE source in a limestone whole-space: experimentally measured values (crosses) from Figure 8 of Murphy et al. (1997); calculated with 1D GEODYN (solid green line); and calculated with 3D WPP (red line for 4-m grid spacing and black line for 1-m grid spacing). These are compared with and the expected geometric spreading for a spherical wave in a homogeneous whole-space (1/R, fine dashed line).

ACKNOWLEDGEMENTS

SEM calculations were performed with the SPECFEM3D package developed by Jeroen Tromp, Dmitri Komatitsch and colleagues and distributed by the Computational Infrastructure for Geodynamics supported by the National Science Foundation (www.geodynamics.org). Calculations were performed on the GNEM Linux cluster, and we are grateful for support by Stan Ruppert and Jenny Aquilino. Larger calculations were performed on massively parallel systems operated by Livermore Computing. WPP was supported in part by Laboratory Directed Research and Development (project 05-ER-079). Some waveform data were obtained from the IRIS Data Management System, which is funded by the National Science Foundation.

REFERENCES

Antoun, T. H., I. N. Lomov and L. A. Glenn (2001). Development and application of a strength and damage model for rock under dynamic loading, proceedings of the 38th U.S. Rock Mechanics Symposium, Rock Mechanics in the National Interest, D. Elsworth, J. Tinucci and K. Heasley (eds.), A. A. Balkema Publishers, Lisse, The Netherlands, 369–374.

Appelo, D. and N.A. Petersson (2008). A stable finite difference method for the elastic wave equation on complex geometries with free surfaces, *Communications in Computational Physics*, in press.

Kennett B.L.N. & Engdahl E.R. (1991). Travel times for global earthquake location and phase identification, *Geophys J Int*. 105: 429–465.

Komatitsch, D. and J.-P. Vilotte (1998). The Spectral Element Method: An efficient tool to simulate the seismic response of 2D and 3D geologic structures, *Bull. Seism Soc. Am*. 88: 368–392.

Komatitsch, D. and J. Tromp (1999). Introduction to the spectral element method for three-dimensional seismic wave propagation, *Geophys. J. Int*. 139: 806–822.

Komatitsch, D., J. Ritsema and J. Tromp (2002). The Spectral-Element Method, Beowolf computing and global seismology, *Science* 298: 1737–1742.

Kustowski B., Ekström G., and A. M. Dziewonski (2008). The shear-wave velocity structure in the upper mantle beneath Eurasia, *Geophys. J. Int.*, in press.

Liu, P.-C. and R. Archuleta (2006). Efficient modeling of Q for 3D numerical simulation of wave propagation, *Bull. Seism. Soc. Am*. 96: 1352–1358.

Liu, Q. and J. Tromp (2006) Finite-frequency kernels based on adjoint methods, *Bull. Seism. Soc. Am*. 96: 2383–2387.

Lomov, I. and M.B. Rubin (2003), Numerical simulation of damage using an elastic-viscoplastic model with directional tensile failure. *Journal De Physique IV*, 110, 281–286.

Murphy, J.R., Kitov, I.O., Rimer, N., Adushkin, V.V., Barker, B.W. (1997) Seismic characteristics of cavity decoupled explosion in limestone: An analysis of Soviet high explosive test data. *Journal of Geophysical Research* 102: (12), 27393–27405.

Nilsson, S., N. A. Petersson, B. Sjogreen and H.-O. Kreiss (2007). Stable difference approximations for the elastic wave equation in second order formulation, *SIAM J. Numer. Anal.* 45: 1902–1936.

Pasyanos, M., G. A. Franz, A. L. Ramirez (2006). Reconciling a geophysical model to data using a Markov chain Monte Carlo algorithm: An application to the Yellow Sea–Korean Peninsula region, *J. Geophys. Res*., Vol. 111, No. B3, B03313, 10.1029/2005JB003851

Pasyanos, M. E., W. R. Walter, M. P. Flanagan, P. Goldstein, and J. Bhattacharyya (2004). Building and testing an *a priori* geophysical model for Western Eurasia and North Africa, *Pure Appl. Geophys.* 161: 235–281

Shapiro, N.M. and M.H. Ritzwoller (2002). Monte-Carlo inversion for a global shear velocity model of the crust and upper mantle, *Geophys. J. Int.* 151: 88–105.

Tromp, J., C. Tape and Q. Liu (2005). Seismic tomography, adjoint methods, time reversal and banana-doughnut kernels, *Geophys. J. Int*. 160: 195–216.

van der Lee, S., S. Chang, M. Flanagan, H. Bedle, F. Marone, E. Matzel, M. Pasyanos, A. Rodgers, B. Romanowicz, and C. Schmid (2007). Joint Inversion for 3-Dimensional S-Velocity Mantle Structure Along the Tethyan Margin, in *Proceedings of the 29th Monitoring Research Review: Ground-Based Nuclear Explosion Technologies*, LA-UR-07-5613, Vol. 1, pp. 312–321.

Vorobiev. O. Y. (2008) Generic strength model for dry jointed rock masses, in press, *International Journal of Plasticity*, 10.1016/j.ijplas.2008.06.009.